Available online at www.sciencedirect.com
SCIENCE DIRECT®
Journal of the European Ceramic Society 25 (2005) 2661–2664
www.elsevier.com/locate/jeurceramsoc

Powder processing, crystalline structure, sintering, and electrical properties of $NdM_{0.5}Mn_{0.5}O_3$ (M = Ni, Co, Cu) manganites

C. Moure [a,*], J. Tartaj [a], V. Gil [a], O. Peña [b], P. Durán [a]

[a] *Instituto de Cerámica y Vidrio (CSIC)-Campus de Cantoblanco, Camino de Valdelatas s/n, 28049 Madrid, Spain*
[b] *Chimie du Solide et Inorganique Moleculaire, UMR 6511, CNRS, Université de Rennes I, Institut de Chimie de Rennes, 35042 Rennes Cedex, France*

Available online 5 May 2005

Abstract

Perovskite single-phase $NdMe_{0.5}Mn_{0.5}O_3$ (Me = Co, Ni, Cu) powders were achieved at low-temperature (600–700 °C) by using the ethylene glycol–metal nitrate polymerized complex method. The structure of the perovskite system was investigated, and an orthorhombic structure O′-type was found for the Co-, Ni-, and Cu-containing perovskite materials. Replacement of Cu, Co, and Ni onto B-sites of the $NdMnO_3$ perovskite structure improve densification of pure manganite up to about 99% of theoretical at temperatures as low as 960 °C in the particular case of the $NdCu_{0.5}Mn_{0.5}O_3$ samples. The sintering enhancement of Cu-, Co- and Ni-containing perovskite materials is explained, assuming the no evidence for a low-temperature eutectic-liquid, as due to a change in the mechanism of the early stages of the densification process.

Keywords: Manganites; Sintering

1. Introduction

Due to their phase stability and thermal expansion compatibility with YSZ in the cofiring process at high temperature, 1300–1400 °C, lanthanum based perovskite systems, i.e., $La_{1-x}A_xMnO_3$ (A = Sr and $x = 0.1$–0.4), have been used as cathode for high temperature SOFC system.[1,2] However, such an asseveration has been strongly questioned by many authors which reported the reaction of the electrolyte YSZ with lanthanum of the perovskite,[3–7] with the formation of a pyrochlore phase $La_2Zr_2O_7$ which ionic conductivity (10^{-4} S cm^{-1}) is three orders lower than that of YSZ (10^{-1} S cm^{-1}) at the SOFC operating temperature (∼1000 °C). For those and many other reasons the last tendencies are addressed to the use of electrolytes, such as those based on doped-ceria, working at temperatures lower than 600–800 °C, and having higher ionic conductivity than YSZ.[8,9] However, such electrolyte has a thermal expansion coefficient much lower than the most of the Co-based perovskite cathodes. Therefore, the search of new compositions having the desirable properties for intermediate temperature SOFC applications is going on.[10]

Many attempts have carried out by substituting a divalent cation (Sr, Ca) for a trivalent cation (La) within A sites of the perovskite structure. Although such a substitution leads to the appearance of electronic holes in air, but a charge compensation of oxygen vacancies, at the same time that a high oxygen flux at moderate overpotentials was expected when using compositions, such as $La_{1-x}Sr_xCo_{1-y}Fe_yO_3$ (LSCFe) as SOFC cathodes. These compositions have demonstrated higher electrical conductivity than LSM and to have high ionic conductivities and, therefore, they are assumed to be as promising SOFC cathode materials.[11–13]

From the above exposed, it could be said that rare earth manganite perovskite oxides have attracted much attention in recent years due to their incorporation as cathodes in high temperature SOFCs, and mainly the composition with La in the A-site have been extensively studied, while much less attention have been given to other rare earth manganites.

The purpose of the present work was to study other rare earth oxide systems as $LnMe_{1-x}Mn_xO_3$, where Ln = Nd and

* Corresponding author. Tel.: +34 91 73 55 843.
E-mail address: cmoure@csic.csic.es (C. Moure).

0955-2219/$ – see front matter © 2005 Elsevier Ltd. All rights reserved.
doi:10.1016/j.jeurceramsoc.2005.03.119

(Me = Co, Ni, Cu) as possible cathode material for intermediate temperature SOFCs. Replacement of lanthanum with neodymium on the A-site, and nickel, cobalt and copper on the B-site of the perovskite structure can provide a more stable system. In a first part, the powder preparation, crystallographic study, and sintering behaviour of the materials prepared by the chemical polymerized complex method, is presented. The effect of Me-doping on these properties was examined.

2. Experimental details

Ceramic powders of the composition $NdMe_{0.5}Mn_{0.5}O_3$ were prepared by the ethylene glycol–metal nitrate polymerized complex process.[14] The powder was calcined at 750 °C for 2 h, and then wet-milled with methanol in an attrition ball milling using zirconia balls. The crystallographic study was made at room temperature by X-ray diffraction (XRD) with a Siemens D5000 diffractometer (Cu Kα radiation) which operated at 40 kV and 30 mA. The XRD data were collected by step scanning in the range $20 < 2\theta < 75$. The lattice parameters were determined using a least squares unit cell refinement computer program.

After drying, the powders also were isostatically pressed (200 MPa). The compacts were then sintered in air by the constant rate of heating (CRH) with a dilatometer (model 402 E/7 Netzsch, Germany), and by the conventional ramp-and-holding methods. The heating and cooling rates were 2 °C/min. The density of the sintered samples was measured by the Archimedes method in water. Microstructure of the samples was observed with a scanning electron microscope (SEM) on the gold-coated polished surfaces.

3. Results and discussion

3.1. Powder characterization

After combustion the material has the black color which remained throughout all the powder processing. The simultaneous TG/DTA curves for the different prepared powder perovskites during heating of the dried polymeric gel between room temperature and 1000 °C, revealed the same thermal features in all cases and, for clarity, only that corresponding to the $NdCu_{0.5}Mn_{0.5}O_3$ perovskite is shown in Fig. 1.

The TG curve showed a total weight loss of about 45% up to 1000 °C, which is due to the evolution of carbon compound as CO or CO_2, and nitrates in the form of N_2, NO, and NO_2. In the DTA curve, the more relevant feature corresponded to that present at about 290 °C, in which an abrupt exothermal peak, almost a line, which is due to the combustion reaction from the decomposition of the polymeric gel, was present.

The ethylene glycol–metal nitrate polymeric gel and calcined powders at different temperatures were also characterized by FTIR, not shown here. However, the appearance of IR

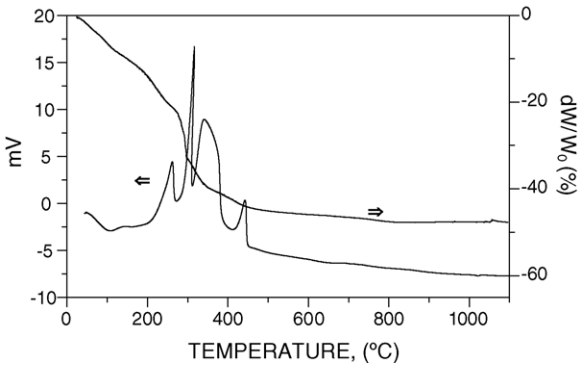

Fig. 1. TG and DTA curves corresponding to the gel precursor of the $NdCu_{0.5}Mn_{0.5}O_3$ composition.

absorption bands at about 2900, 1730, 1640 and 1400–1300, 1380,1330,1090–1040, and 500 cm^{-1} are related to CH and CH_2 stretches, C=O stretching of residual acid groups, carbonaceous materials, NO_3^- ion stretching, OH or C–OH stretches, symmetric and antisymmetric stretches of C–O, and metal–oxygen bonds, respectively.[15] In the final reacted powders, most of these IR bands disappeared, and only those assigned to the metal–oxygen bonds were still observed.

Fig. 2 shows the XRD patterns of the dried polymeric gel, after the combustion reaction, and after calcining. The

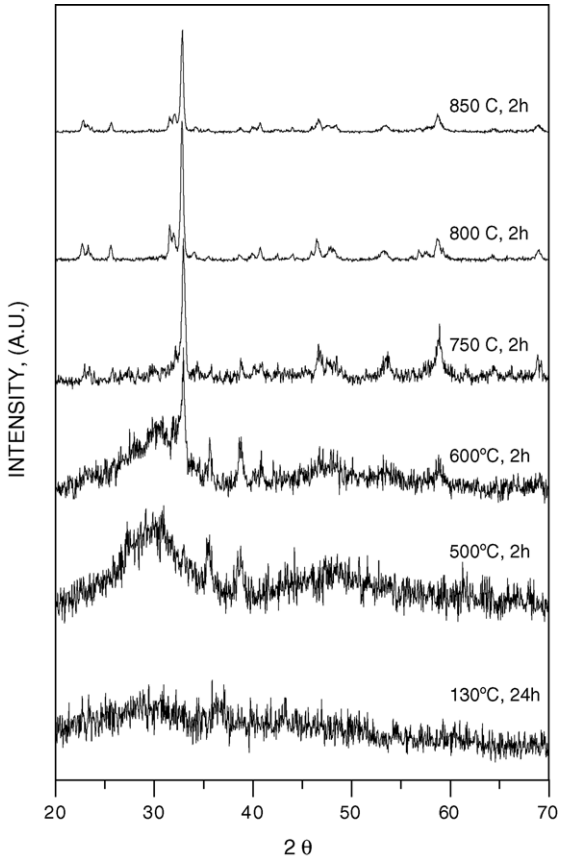

Fig. 2. Evolution of X-ray patterns of the polymerized gel corresponding to the Cu composition, as a temperature function.

Table 1
Phase symmetry, lattice parameters, unit cell volume, orthorhombicity, and type of orthorhombic structure of the $NdMe_{0.5}Mn_{0.5}O_3$ manganites

Samples	Symmetry	a (nm)	b (nm)	c (nm)	Volume (nm^3)	b/a	Type of orthorhombic structure
$NdMnO_3$	Orthorhom	0.5408	0.5788	0.7555	0.2364	1.07	O′-type
$NdNi_{0.5}Mn_{0.5}O_3$	Orthorhom	0.5428	0.5560	0.7510	0.2267	1.024	O′-type
$NdCo_{0.5}Mn_{0.5}O_3$	Orthorhom	0.5433	0.5579	0.7527	0.2281	1.027	O′-type
$NdCu_{0.5}Mn_{0.5}O_3$	Orthorhom	0.5429	0.5564	0.7599	0.2297	1.025	O′-type

Pure Nd manganite is included for comparison.

polymeric gel was amorphous and remained as such after the combustion reaction, i.e., the perovskite phase was not formed up to higher temperatures (>600 °C) indicating, thus, that the temperature reached during the ignition was not sufficient to crystallize the perovskite phase. After calcining at 750 °C a well-crystallized perovskite phase was obtained and all the diffraction peaks could be indexed according to an orthorhombic *Pbnm* space group ($GdFeO_3$-type structure). The crystallographic data for the three synthesized perovskite phases are given in Table 1. As it is well known, two types of orthorhombic structures are generally distinguished. The O-type structure, which is characterized by the relationship $a \leq c/(2)^{1/2} \leq b$, exists when the lattice deformation is relatively small, while the O′-type structure, with $c/(2)^{1/2} \leq a \leq b$, exists in the case of a relatively enhanced lattice deformation. According to these crystallographic data, it can be said that the lattice deformation by the replacement of Mn by the transition metal, such as Co, Ni, and Cu on the B-site of the perovskite structure was relatively small. The existence of an O′-type structure in the three perovskite material, i.e., the same as in the pure $NdMnO_3$, supported such a statement. On the other hand, the orthorhombicity factor, b/a, is closer to unity in the sequence Co > Ni > Cu. We, further, assume a particle coordination number of 6 in all cases and, therefore, the cationic radius size[16] sequence Co^{2+} (0.745 Å) > Cu^{2+} (0.73 Å) > Ni^{2+}.(0.69 Å) > Mn^{3+} (0.645 Å) is in some contradiction with the above b/a variation.

The specific surface areas measured by the nitrogen adsorption, using a three point BET analysis, were 13.5, 20, and 10 $m^2\,g^{-1}$ after calcining at 750 °C for 2 h. The particle (agglomerate) size calculated from the BET analysis using the equation $d_{BET} = 6/S\rho$, where ρ is the crystallographic density of the powder were about 62, 41, and 82 nm for the perovskite powders $NdCo_{0.5}Mn_{0.5}O_3$, $NdNi_{0.5}Mn_{0.5}O_3$, and $NdCu_{0.5}Mn_{0.5}O_3$, respectively. These results indicated: (a) that this synthesis method successfully leads to perovskite single-phase powders and (b) the obtained powders are in the nanosize range and, therefore, they are highly sinterable.

3.2. Sintering and microstructural development

Green compacts were prepared from powders calcined at 750 °C and sintered up to 1450 °C in air, by the CRH method. Fig. 3 shows the linear shrinkage rate ($d(dL/L_o)/dT$) as a function of temperature for the different perovskite materials.

It can be observed from this figure that the substitution of Mn by Cu in the perovskite structure shifts the onset of sintering towards lower temperatures than with Co or Ni and, moreover, the addition of Cu decreases the temperature of maximum shrinkage rate (T_m) significantly. For example, T_m decreases from 1300 °C for pure $NdMnO_3$ perovskite to 960 °C for $NdCu_{0.5}Mn_{0.5}O_3$, i.e., almost 350 °C lower. In the case of the Co substitution such a decreasing in T_m was of only 100 °C, and in the case of Ni substitution Tm was slightly higher than that for the pure perovskite material. Furthermore, it must be noted that the width of the shrinkage temperature range also decreases, and for Cu-, Co-, and Ni-containing perovskite materials is much narrower. Such a behaviour could be considered as a typical phenomenon present in a liquid phase-assisted densification process,[17] at least, in the case of the Cu and Co replacement. However, the no evidence for a low-temperature eutectic point in the Nd–Me–Mn ternary oxides system, is suggesting that the fast densification rate in Cu-, and Co-perovskite materials could not be related to liquid-phase sintering and, therefore, another different mechanism predominates, at least in the early stages of sintering.

The microstructure of the $NdNi_{0.5}Mn_{0.5}O_3$ sample sintered at 1450 °C (90% dense), as shown in the Fig. 4a was very uniform, with a small grain size (~1 μm). Fig. 4b shows the microstructure of the $NdCo_{0.5}Mn_{0.5}O_3$ sample after sintering at 1350 °C (94% dense). Many trapped pores within the grains were present as consequence of the oxygen loss during the reduction process of Co_3O_4 to CoO at high temperatures. At higher magnification, no shown here, a twinning domain phenomenon on the grain surfaces was present, which is typical of a structure transition occurring on cooling. The grain

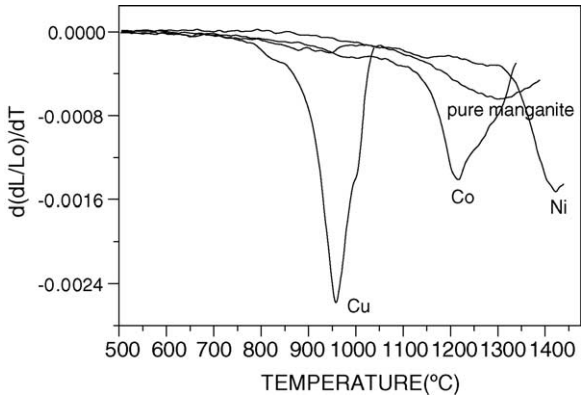

Fig. 3. Linear shrinkage rate as a function of temperature for the different perovskite materials.

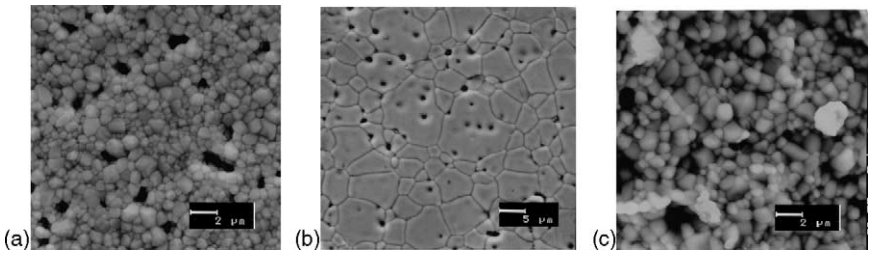

Fig. 4. Micrographies of sintered samples: (a) Ni sample; (b) Co sample; (c) Cu sample.

size was ∼5 μm, with a quite uniform grain size distribution. $NdCu_{0.5}Mn_{0.5}O_3$ sample sintered at 1000 °C, (98% dense) did not shows any twinning phenomenon and the grain size was quite small, (∼1.5 μm), as it is shown in the Fig. 4c. From these microstructural features it can be said that the Ni^{2+} cations inhibited the grain growth process.

4. Conclusions

Perovskite single-phase $NdMe_{0.5}Mn_{0.5}O_3$ (Me = Co, Ni, Cu) powders were achieved at low-temperature (600–700 °C) by using the ethylene glycol–metal nitrate polymerized complex method. The structure of the perovskite system was investigated, and an orthorhombic structure O′-type was found for the Co-, Ni-, and Cu-containing perovskite materials. Replacement of Cu, Co, and Ni onto B-sites of the $NdMnO_3$ perovskite structure improve densification of pure manganite up to about 99% of theoretical at temperatures as low as 960 °C in the particular case of the $NdCu_{0.5}Mn_{0.5}O_3$ samples. The sintering enhancement of Cu-, Co-, and Ni-containing perovskite materials is explained, assuming the no evidence for a low-temperature eutectic-liquid, as due to a change in the mechanism of the early stages of the densification process.

Acknowledgement

The present work was supported by Project 07N/0096/02 of the Autonomous Community of Madrid (CAM).

References

1. Minh, N. Q., Ceramic fuel cells. *J. Am. Ceram. Soc.*, 1993, **76**, 563.
2. Yamamoto, O., Takeda, Y., Kanno, R. and Kojima, T., Perovskite-type oxides as oxygen electrodes for high temperature solid oxide fuel cells. *Solid State Ionics*, 1987, **22**, 241.
3. Lau, S. K. and Singhal, S. C., Potential electrode/electrolyte interactions in solid oxide fuel cells. *Corrosion*, 1985, **85**, 345, Boston, MS.
4. Taimatu, H., Wada, K. and Kaneko, H., Mechanism of reaction between lanthanum manganite and YSZ. *J. Am. Ceram. Soc.*, 1992, **75**, 401.
5. Yokokawa, H., Saka, N., Kawada, T. and Dokiya, M., Thermodinamic analysis on interface between perovskite electrode and YSZ electrolyte. *Solid State Ionics*, 1990, **40–41**, 398.
6. Yamamoto, O., Takeda, Y., Kanno, R. and Kojima, T., Stability of perovskite oxide electrode with stabilized zirconia. In *Proceedings of the First Internal Symposium on SOFCs*, ed. S. C. Singhal, 1989, p. 242.
7. Takeda, Y., Nakai, S., Kojima, T., Kanno, R., Imanishi, N., Shen, G. D. *et al.*, Electrical and mechanical properties of zirconia-alumina composite electrolyte. *Mater. Res. Bull.*, 1991, **26**, 153.
8. Mogensen, M., Lindegaard, T. and Hansen, U. R., Physical properties of mixed conductor solid oxide fuel cell anodes of doped CeO_2. *J. Electrochem. Soc.*, 1994, **41**, 2122.
9. Navarro, L. M., Marques, F. M. B. and Frade, J. R., n-Type conductivity in Gadolinia-doped ceria. *J. Electrochem. Soc.*, 1997, **144**, 267.
10. Carter, S., Selcuk, S., Chater, R. J., Kajda, J. and Kilner, J. A., Oxygen transport in selected nonstoichiometric perovskite-structure oxides. *Solid State Ionics*, 1992, **53–56**, 597.
11. Tai, L. W., Nasrallah, M. M., Anderson, H. U., Sparlin, D. M. and Schlin, S. R., Structure and electrical properties of $La_{1-x}Sr_xCo_{1-y}Fe_yO_3$. Part I. The system $La_{0.8}Sr_{0.2}Co_{1-y}Fe_yO_3$. *Solid State Ionics*, 1995, **76**, 259.
12. Tai, L. W., Nasrallah, M. M., Anderson, H. U., Sparlin, D. M. and Schlin, S. R., Structure and electrical properties of $La_{1-x}Sr_xCo_{1-y}Fe_yO_3$, Part II. *Solid State Ionics*, 1995, **76**, 273.
13. Maguirre, E., Gharbage, B., Marques, F. M. B. and Labrincha, J. A., Cathode materials for intermediate temperature SOFCs. *Solid State Ionics*, 2000, **127**, 329.
14. Duran, P., Tartaj, J., Rubio, F., Peña, O. and Moure, C., Preparation and powder characterization of spinel-type $Co_xNiMn_{2-x}O_4$ ($0.2 < x 1.8$) by the ethylene glycol–metal nitrate polymerized complex process. *J. Eur. Ceram. Soc.*, 2004, **24**, 3035.
15. Nakamoto, K., *Infrared and Raman Spectra of Inorganic and Coordination Compounds* (*4th ed.*). Wiley, New York, 1986.
16. Shanon, R. D. and Prewitt, C. T., Effective ionic radii in oxides and fluorides. *Acta Crystallogr. A*, 1976, **32**, 751.
17. Kingery, W. D., Bowen, H. K. and Uhlmann, D. R., *Introduction to Ceramics* (*2nd ed.*). Wiley, New York, 1976.